OPEN ACCESS

Kashf Journal of Multidisciplinary Research
Vol: 03 - Issue 01 (2026)
P-ISSN: 3007-1992 E-ISSN: 3007-200X
https://kjmr.com.pk

FTIR SPECTROSCOPIC INVESTIGATION OF CO-PRECIPITATED ZNO–TIO₂ NANOCOMPOSITES: VIBRATIONAL FEATURES, METAL–OXYGEN BONDING, AND INTERPRETIVE LIMITATIONS

Muhammad Waqar Anwar[1], Zahir Hussain[1], Maryam Mushtaq[1], *Kanwal Akhtar[1, 3], Muhammad Khawar Abbas[2]

[1]*Faculty of Sciences, The Superior University Lahore, Pakistan.*

[2]*Department of Physics, Government College University, Faisalabad, Pakistan.*

[3]*Department of Physics, Government College Women University, Faisalabad, Pakistan.*

[*]***Corresponding Author:*** (kanwal.akhtar.fsd@superior.edu.pk)

DOI: (*https://doi.org/10.71146/kjmr744*)

Article Info

This article is an open access article distributed under the terms and conditions of the Creative Commons Attribution (CC BY) license https://creativecommons.org/licenses/by/4.0

Abstract

Zinc oxide (ZnO) and titanium dioxide (TiO_2) are common inorganic UV-filter ingredients, and composites holding both oxides have been investigated for their potential optical and surface properties. A co-precipitated ZnO–TiO_2 sample S1 is prepared using 6.813 g $ZnCl_2$, 1.000 g pre-formed TiO_2 and 8.000 g of NaOH and its Fourier-transform infrared (FTIR) transmittance spectrum is examined. The sample was dried but was not calcined. The spectra were taken between 4000 and 650 cm -1. No well-resolved sample-related absorption bands were observed above approximately 1000 cm^{-1}. Features near 3900–3500 cm^{-1} and 1750–1400 cm^{-1}, and also one near 2360 cm^{-1}, were interpreted as being due to water-vapour and CO_2 in the atmosphere. Transmittance values were significantly reduced < ~1000 cm-1 with a low limit of detection of ~50% at the lowest transmittance measured. This is in line with the high absorption values obtained in the metal–oxygen related vibration, and the absorption minimum was not resolved, nor were the contribution of the metal–O and the oxygen–H vibrations resolved individually. The contributions of hydroxyl, adsorbed-water, and carbonate species were neither confirmed nor ruled out. The absorption at low wavenumbers is then tentatively interpreted in the available spectrum, with the need for further measurements to determine the phase composition and surface chemistry of the material.

Keywords:

ZnO–TiO_2 composite; FTIR spectroscopy; co-precipitation; metal–oxygen vibrations; surface hydroxyl groups; UV-filter materials.

Highlights

- The FTIR transmittance spectrum of the co-precipitated ZnO–TiO_2 sample was studied in the range of 4000–650 cm^{-1}.
- Observed spectral features are distinguished from proposed interpretations.
- The sharp drop in transmittance below about 1000 cm-1 is in accord with the absorption due to metal–oxygen bonding; its minimum lies outside the measured range.

The contribution of possible hydroxyl and adsorbed-water and carbonate contributions are not resolved.

1. Introduction

1.1 Ultraviolet radiation and mineral sunscreens

Solar ultraviolet (UV) radiation that reaches the Earth's surface is often split into ultraviolet B (UV-B; ~290-320 nm) and ultraviolet A (UV-A; ~320-400 nm). Sunscreen products are intended to protect over the designated UV spectrum [1,2]. Common inorganic UV-filter ingredients are titanium dioxide (TiO_2) and zinc oxide (ZnO). They have different optical responses and it has been suggested that using these together is one method of achieving extensive coverage of UV attenuation [2,3]. However, the exact performance of a sunscreen is related to the characteristics of the material and formulation and cannot be deduced from FTIR data only.

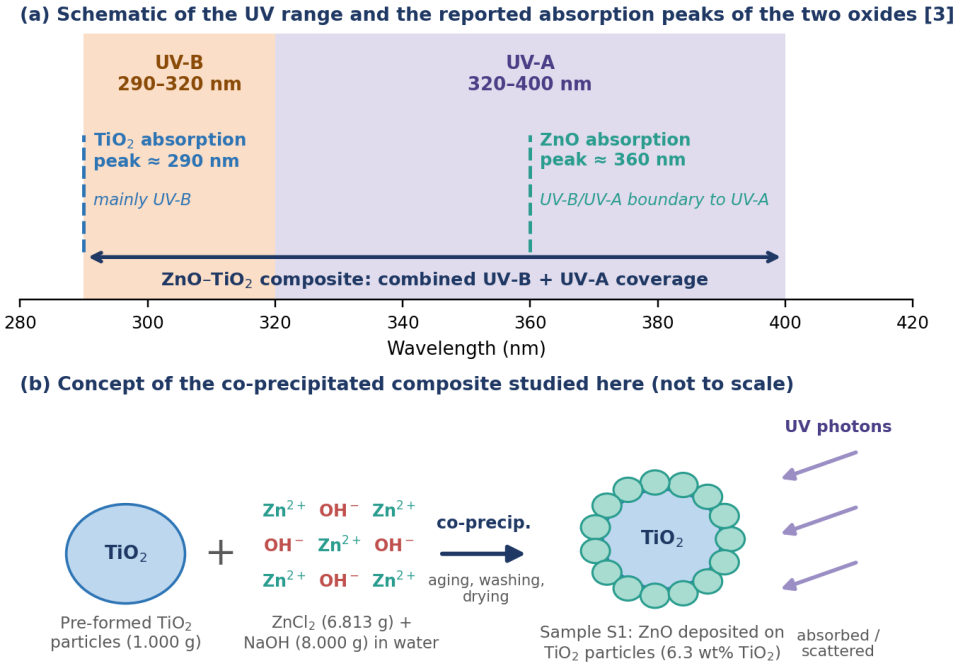


Figure 1: Introductory schematic. **(a)** UV-B and UV-A range and literature-reported absorption features of TiO_2 and ZnO [3] are shown in the diagram. **(b)** Conceptual illustration of the intended co-precipitation route is a precipitate containing zinc is formed in the presence of pre-formed TiO_2 particles.

1.2 Particle size, appearance, and free-radical considerations

Conventional mineral sunscreens made with relatively large particles of oxides may be white or opaque. Reduction of the particle size can change the UV attenuation and hence the optical properties of these materials, but it can also impact the surface activity and formulation properties [2,4]. The effects of particle processing on the production of free radicals and on UV protection have been studied previously [3]. The findings here should be interpreted as representative of the performance of the particles and processing conditions and are not intended to represent the performance of the sample used in the present study.

1.3 ZnO–TiO_2 composites as UV filters

Combining ZnO and TiO_2 in a composite has been investigated as a way to modify UV attenuation and particle architecture. Zinc Oxide–TiO2 composites, produced by dry nanodispersion, showed improved UV-absorption properties by Reinosa et al. [6] and subsequent studies focused on hierarchical composites with a focus on balancing the properties of UV-protection and photodegradation [7]. Additionally, ZnO–TiO_2 formulations for use in sunscreens have been studied [3,8]. These reports are only context for the current material and are not considered to provide a measure of the UV-filter performance of Sample S1 in this study.

1.4 Co-precipitation and surface chemistry

Wet co-precipitation can be used to form zinc-containing precipitates in the presence of pre-formed TiO_2. During precipitation, the chemical species of zinc hydroxide or basic zinc carbonate may be formed, which can remain in the product when it is dried without calcination under the conditions of the solution chemistry and processing conditions [9,10]. Oxide powders' surface properties can be modified by surface hydroxyl, adsorbed water and carbonate species. However, in S1, their presence has to be established from appropriate measurements and not entirely from the synthesis route.

1.5 FTIR spectroscopy of ZnO and TiO_2

FTIR spectroscopy is used to study vibrations which are associated with the change of dipole moment. Typically, metal–oxygen related absorption is present in the lower wavenumber range in oxide materials, whilst hydroxyl groups and adsorbed water can contribute at the higher wavenumber range. There are indications of Zn–O-related bands at 568 cm^{-1} and 465 cm^{-1} as well as the presence of broad Ti–O/Ti–O–Ti absorption bands over the range of about 400–1000 cm^{-1} as reported in literature, but with different positions depending on the structure of the materials and conditions of investigation [12,13]. The spectrum covered in this study is limited to 650 cm^{-1}, which is not adequate to resolve all potentially relevant metal–oxygen features.

1.6 Objective and scope

The transmittance spectrum of one co-precipitated sample that was prepared with 1.000 g of TiO_2 (6.32 wt% of the total amount of the initial precursor) is investigated in this study. This percentage is a nominal loading, based on the precursor, and not a composition of the final powder. The goal is to differentiate between the definitive features of the spectrum and the tentative features, as well as to explain the shortcomings of the spectrum that is available and to outline measurements that would help to characterize it more accurately. This study is not meant to provide evidence for better UV protection, sunscreen performance or to achieve statistical significance.

2. Materials and Methods

2.1 Materials

The chemicals used were zinc chloride ($ZnCl_2$), titanium dioxide (TiO_2) powder, sodium hydroxide (NaOH), and distilled water. The TiO_2 was used as a pre-formed oxide powder and was not further purified. This information should be included if available in the laboratory records: supplier, purity and the phase of the TiO_2.

2.2 Synthesis of sample S1

The sample S1 was prepared with the addition of NaOH to the solution that contains the dispersed TiO_2 and $ZnCl_2$. In distilled water, 6.813 g of $ZnCl_2$ (about 0.050 mol) was dissolved under magnetic stirring and 1.000 g of TiO_2 was dispersed in the solution. The solution of NaOH was prepared from 8.000 g of NaOH (which is about 0.200 mol) and added dropwise with continuous stirring up to the point of no precipitate was reported. The precipitate was stirred for 30 min in the mother liquor, filtered, washed with a number of distilled water and then dried in a laboratory oven for 30 min and ground to powder. No information was provided on water volume, reaction temperature, addition rate, pH, washing endpoint, drying temperature in the manuscript supplied, and these should be inserted from the laboratory record. Since the amount of NaOH used is about twice the one required in the simplified reaction for the formation of $Zn(OH)_2$ from 0.050 mol of $ZnCl_2$, the chemical identity of the final solid product should not be assumed to be pure ZnO without supporting characterization.

Figure 2: Flowchart of the reported preparation and FTIR characterization of Sample S1.

Table 1. Preliminary precursor mixture used to make Sample S1.

Component	Mass (g)	Amount (mol)	Share of precursor mass (wt%)
$ZnCl_2$	6.813	0.050	43.1
TiO_2	1.000	_	6.3
NaOH	8.000	0.200	50.6
Total	15.813	–	100.0

2.3 Principle of the FTIR measurement

An infrared-active vibrational mode absorbs radiation when the vibration frequency of a mode is equal to the frequency of the radiation, and the vibration changes the dipole moment, then the radiation is absorbed. Generally, absorption appears as a reduction in transmittance in a transmittance spectrum. The vibrations of metal–oxygen bonds can be found at lower wavenumbers while O–H stretching and water-related vibrations can be found at higher wavenumbers. These ranges have been included for interpretation and not as proof of a specific chemical species.

2.4 FTIR measurement

A FTIR spectrum was measured from 4000-650 cm^{-1} and the background spectrum was measured prior to the sample measurement.

$$T\ (\%) = (I / I_o) \times 100 \quad (1)$$

I is the intensity transmitted by the sample and I_0 is the intensity in the blank. Absorbance can be determined from the transmittance T in percent as:

$$A = -\log_{10}(T / 100) \quad (2)$$

2.5 Data processing and uncertainty

The approximate transmittance values were read from the calibration curve generated from the instrument, therefore mapping the curve to the plotted axes. The manuscript gives the uncertainty level as ±10 centimetres^{-1} in wavenumber and ±1 per cent in transmittance. These estimates are only provisional and may fail to account for all the sources of uncertainty in the graph extraction process. The best option is to get and analyze the original numeric data file.

$$\Delta T = T(1300\ cm^{-1}) - T(655\ cm^{-1}) \quad (3)$$

No repeatability analysis or between-sample variability could be estimated as only one spectrum was analyzed.

3. Results

The FTIR transmittance spectrum of Sample S1 is shown in figure 3 below. The main features of the spectrum, as noted by the principal, are tabulated in Table 2 and approximate transmittance values are tabulated in Table 3.

Figure 3: FTIR transmittance spectrum of sample S1 obtained in the range 4000 - 650 cm^{-1}. Transmittance (%) is shown as a function of wavenumber (cm-1). The numbers obtained from the graph are approximate.

The transmittance of the spectrum was relatively high throughout the range of measurements. There was no well-defined sample-related absorptive band detected on the upper end of the spectrum above about 1000 cm-1. Between about 3300 and 2000 cm^{-1}, transmittance increased gradually from approximately 91% to 97%. Features seen in the areas around 3900–3500 and 1750–1400 cm^{-1} were narrow, and a small feature was seen near 2360 cm^{-1}. A low intensity depression around 1500-1400 cm-1 was detected. Transmittance decreased below 1300 cm^{-1}, with a shoulder at 900-950 cm^{-1} and a more rapid decline at lower wavenumbers. The transmittance was about 60% around 778 cm^{-1} and about 50% at the lower limit of the spectral range measured. The minimum of the spectrum was not recorded as the spectrum terminated at 650 cm^{-1}.

Table 2. Results of the observed FTIR features of Sample S1 and interpretation.

Region (cm^{-1}, ±10)	Observation	Proposed origin	Basis	Needs literature confirmation?
3900–3500	Narrow irregular lines	Atmospheric water vapor (rotation–vibration)	Sharp, closely spaced lines; no broad envelope	Yes; confirm with purged background
~2360	Small narrow feature	Atmospheric CO_2 (ν_3 region)	Characteristic position and narrow shape	Yes
3400–3200 (broad)	Flat ~90–91 %T, then smooth rise	Weak broad O–H absorption not excluded; not separable from baseline	No band edge or maximum resolved; O–H of ZnO reported at 3441 and 3105 [12]	Yes; unresolved
1500–1400	Shallow broad depression, ~91.5 %T, with vapor lines on it	Carbonate ν_3, hydroxyl or adsorbed water, or vapor only	Hydrozincite ν_3 at 1515 and 1383 [10]; overlap with vapor lines	Yes; unresolved
900–950	Shoulder on descending edge	Not assigned	Depends on phase composition	Yes
<1000 to 650	Steep fall in %T; no minimum	Metal–oxygen lattice absorption (Zn–O, Ti–O–Ti), maximum below 650 cm^{-1}	Zn–O at 568 and 465 [12]; Ti–O–Ti 400–1000 [13]	Yes; band positions not located

Table 3: Approximate transmittance values read from Figure 3 (estimated uncertainty: ±10 cm^{-1} in wavenumber and ±1 percentage point in transmittance).

Wavenumber (cm^{-1})	T (%)	Region
3800	90.8	Vapor-line region
3500	90.4	Vapor-line region
3000	93.1	Baseline
2000	96.7	Baseline
1630	94.0	No isolated feature
1500	91.6	Shallow depression

Wavenumber (cm^{-1})	T (%)	Region
1300	93.5	Local maximum
1000	87.2	Onset of edge
900	83.2	Shoulder
800	64.6	Edge
700	50.8	Edge
655	50.1	Range limit
ΔT, Eq. (3)	43.4	Strength of low-wavenumber absorption

4. Discussion

The discussion distinguishes direct observations from tentative interpretations. Band positions reported in the literature (Table 4) are not measured in the present study, but are values taken from cited literature. Assignments should be qualitative, because the spectrum is extracted from a plotted image and is not available at wavelengths below 650 cm-1.

Table 4. Literature-reported band positions used for comparison; these values were not measured in the present study.

Species / mode	Reported position (cm^{-1})	Material and source
Zn–O stretching	568 and 465	ZnO quantum dots, FTIR [12]
Zn–O vibration	501	ZnO-doped liquid-crystal system [12]
O–H stretching (broad)	3441 and 3105	ZnO nanoparticles [12]
Antisymmetric CO_3^{2-} stretching (ν_3)	1515 and 1383	Hydrozincite, synthetic and natural [10]
OH vibrations	3234, 3303 and 3363	Hydrozincite [10]
Ti–O, Ti–O–Ti (broad)	about 400–1000	TiO_2-containing biocomposite [13]

4.1 Atmospheric contributions

The narrow features in the spectral regions around 3900–3500 cm^{-1} and 1750–1400 cm^{-1}, together with the feature near 2360 cm^{-1}, could be due to contributions from atmospheric water vapour and CO_2 which may not have been cancelled by subtracting the background and the sample scans. Spectrum alone does

not prove the attribution. Repeated measurements with a new background and (when available) a purged sample compartment would aid the evaluation of these features.

4.2 Hydroxyl groups and adsorbed water

Typical regions for the O–H stretching vibrational bands of hydroxyl groups and adsorbed water are around 3500–3000 cm^{-1} and around 1600–1650 cm^{-1} for the bending mode of water, respectively. No well-defined broad O–H band, or any isolated feature near 1630 cm^{-1} was detected for Sample S1. A weak contribution from the surface O–H or from the adsorbed water is difficult to evaluate due to the gradual baseline trend and to the potential contribution from the atmosphere. But these species can't be confirmed or excluded from the spectrum available.

4.3 The 1500–1400 cm^{-1} depression and a possible carbonate contribution

The shallow depression in the 1500 - 1400 cm^{-1} region could result from a number of different causes. The bands of carbonate-related species have been reported around 1515 and 1383 cm-1 [10] and carbonate species can be chemically formed under alkaline precipitation conditions [9]. The feature in S1 however is weak and has a region affected by narrow atmospheric features. The present spectrum thus does not prove the presence of carbonate. This possibility could be investigated by further FTIR measurements and by complementary phase or thermal analysis.

4.4 Metal–oxygen absorption below 1000 cm^{-1}

The most noticeable spectral difference was the decrease in transmittance below about 1000 cm-1, through to the 650 cm-1 measurement limit. This is consistent with strong absorption which is characteristic of metal–oxygen lattice vibrations. Zn–O-related features are reported in the range of 568 and 465 cm^{-1} [12,13] while Ti–O/Ti–O–Ti absorption in the range of 400–1000 cm^{-1} was reported. The measured spectrum is not however deepening to the absorption minimum, and the position and relative contribution of individual bands cannot be established. The data do not also provide any evidence for the presence of interfacial Zn–O–Ti bonds. The transmittance value at the lower measurement limit should be compared to the original plot or numerical data before submitting.

4.5 Baseline

The overall trend of increasing transmittance from about 3300 to 2000 cm- 1 was not considered to be a resolved vibrational band. Sample scattering, thickness, contact or other instrumental and/or processing effects are potential causes.

4.6 Relevance for sunscreen formulation

Surface hydroxyl groups, adsorbed water, and carbonate species can be relevant to the dispersion and surface behaviour of oxide powders. The present FTIR spectrum, however, does not allow for any conclusions to be made with respect to the surface chemistry of Sample S1, nor were any conclusions made in terms of UV–visible absorption, SPF or photostability measurements. In this study, the suitability or effectiveness of material as a sunscreen ingredient is therefore not tested.

4.7 Limitations

Some of the drawbacks were: (i) the spectrum does not reach the absorption minimum at lower wavenumbers, (ii) some spectral regions are hampered by the presence of atmospheric features, (iii) the values have been estimated from a plotted spectrum and not exported as numerical data, (iv) only one spectrum of one sample was analyzed, (v) the spectrum could not be compared to the spectrum of pure ZnO or other TiO_2 loadings, and (vi) the spectrum does not enable the crystalline phases present in the final material to be determined. The conditions for the synthesis also need to be explained and the phase composition of the final solid needs to be checked.

5. Conclusion

The FTIR spectrum of the Sample S1 revealed a sharp drop in transmittance below ~1000 cm-1, characteristic of metal–oxygen absorption. Narrow features in several higher wavenumber regions were interpreted as being from atmospheric water-vapour and CO_2 contribution, with possible hydroxyl and adsorbed-water and carbonate features unresolved. The spectrum was incomplete up to 650 cm-1 and the data was estimated from a graph, and therefore individual metal–oxygen bands could not be identified. The results available are not a proof of the composition of the crystalline phases present in the product or of the UV-filtering properties. More measurement is needed before more confident chemical or application related conclusions can be drawn.

6. Limitations and Future Work

Future work should begin by verifying the synthesis conditions and establishing the phase composition of the final solid, for example by X-ray diffraction where appropriate. If the instrument allows, redo the FTIR measurement with the instrument settings noted, a new background scan, and a measurement down to about 400 cm-1. Numerical data and replicate measurements should be reported if exported. Comparing with the initial TiO_2 and appropriate zinc-containing controls, as well as with samples made at a variety of nominal TiO_2 loading, would aid in the clarification of the differences in the spectra. If the performance of the UV filters is to be assessed then suitable UV–visible and sunscreen-performance measurements would be necessary.

References

[1] Burnett, M. E., & Wang, S. Q. (2011). Current sunscreen controversies: a critical review. *Photodermatology, photoimmunology & photomedicine*, *27*(2), 58-67.

[2] Smijs, T. G., & Pavel, S. (2011). Titanium dioxide and zinc oxide nanoparticles in sunscreens: focus on their safety and effectiveness. *Nanotechnology, science and applications*, 95-112.

[3] Yang, P., Wang, H., Chen, Y., Li, Y., Zhang, J., Zhang, C., ... & Wei, X. (2023). Ball-milling of titanium dioxide and zinc oxide for enhanced UV protection. *Frontiers in Materials*, *10*, 1273659.

[4] Surber, C., Plautz, J., Dähnhardt-Pfeiffer, S., & Osterwalder, U. (2021). Size Matters! Issues and Challenges with Nanoparticulate UV Filters. *Current Problems in Dermatology*, *55*, 203-222.

[5] Lee J-H, Lee G-S, Park E-N, Jo D-H, Kim S-W, Lee H-C. Synthesis of planar-type ZnO powder in non-nano scale dimension and its application in ultraviolet protection cosmetics. Materials 2023; 16(5): 2099. doi:10.3390/ma16052099

[6] Reinosa, J. J., Leret, P., Álvarez-Docio, C. M., del Campo, A., & Fernández, J. F. (2016). Enhancement of UV absorption behavior in ZnO–TiO2 composites. *boletín de la sociedad española de cerámica y vidrio*, *55*(2), 55-62.

[7] Reinosa, J. J., Docio, C. M. Á., Ramírez, V. Z., & Lozano, J. F. F. (2018). Hierarchical nano ZnO-micro TiO2 composites: High UV protection yield lowering photodegradation in sunscreens. *Ceramics International*, *44*(3), 2827-2834.

[8] Siswanto, Qulub, F., & Ofelia Viannco Junico, V. (2025, January). Nanoparticle formulation of ZnO: TiO2 as sunscreen cream for Cutaneous Lupus Erythematosus (CLE) patients. In Journal of physics: conference series (Vol. 2945, No. 1, p. 012019). IOP Publishing.

[9] Sigoli, F. A., Davolos, M. R., & Jafelicci Jr, M. (1997). Morphological evolution of zinc oxide originating from zinc hydroxide carbonate. *Journal of Alloys and Compounds*, *262*, 292-295.

[10] Sanna, R., De Giudici, G., Scorciapino, A. M., Floris, C., & Casu, M. (2013). Investigation of the hydrozincite structure by infrared and solid-state NMR spectroscopy. *American Mineralogist*, *98*(7), 1219-1226.

[11] Tamanna, N. J., Hossain, M. S., Tabassum, S., Bahadur, N. M., & Ahmed, S. (2024). Easy and green synthesis of nano-ZnO and nano-TiO2 for efficient photocatalytic degradation of organic pollutants. *Heliyon*, *10*(17).

[12] Singh, A. K., & Singh, S. P. (2024). Formation of nano and micro scale hierarchical structures in MgO and ZnO quantum dots doped LC media: The role of competitive forces. *arXiv preprint arXiv:2401.09335*.

[13] Konuk Ege, G., Bahar Okuyucu, M., & Akay Sefer, Ö. (2025). Electrospun PANI/PEO-Luffa cellulose/TiO2 nanofibers: a sustainable biocomposite for conductive applications. *Polymers*, *17*(14), 1989.